Conformational Change and Inactivation of Membrane Phospholipid-Related Activity of Cardiotoxin V from Taiwan Cobra Venom at Acidic pH†

Chien-Min Chiang, Kun-Yi Chien, Hai-jui Lin, Ji-Fu Lin, Hsien-Chi Yeh, Pei-li Ho, and Wen-guey Wu*

Department of Life Sciences, National Tsing Hua University, Hsinchu, Taiwan 30043

Received November 29, 1995; Revised Manuscript Received May 6, 1996⊗

ABSTRACT: The phospholipid binding activity of cardiotoxin V from *Naja naja atra* (CTX A5) was studied by use of Langmuir monolayers and found to exhibit pH-dependence in binding to phosphatidylcholine membrane with an apparent pK_a around 6.0. Proton NMR investigation of the CTX A5 molecule in the presence of phosphatidylcholine micelles reveals a decrease in association of CTX A5 with membranes at low pH as a result of the protonation of His-4 near the membrane binding site of loop I region of CTX. The pH-dependent binding can be attributed mainly, but not solely, to the change in charge content of the CTX molecule upon His-4 protonation at the membrane/water interface. This is shown by analyzing the pH- and ionic strength dependence of binding of CTXs to phospholipid monolayers according to Gouy−Chapman theory. The protonation of the His-4 residue also results in a local conformational change in the loop I region since the chemical shifts of amide protons for the amino acid residues from Cys-3 to Thr-14 are all found to vary as a function of pH with an apparent pK_a similar to that of His-4. Interestingly, the effect is relayed to other amino acid residues in the structural core of the protein such as those in C-terminal (Lys-60, Cys-61, and Asn-62) and triple-stranded antiparallel β-sheet (Cys-22, Lys-24, Ala-25, Arg-38, and Ala-41) regions. An additional local conformational change in the molecule results around pH 5 as evidenced by circular dichroism spectroscopic studies, although this change does not affect the characteristic β-sheet and three-finger loop structure of CTX molecule as revealed by two-dimensional NOESY ^{1}H NMR study. The latter conformational change at acidic pH, however, completely inactivates CTX-induced aggregation/fusion activity of sphingomyelin vesicles. The results suggest that deciphering the functional sites of CTXs on the basis of structure and dynamics determined at low pH should be done with caution. Since 19 out of 44 CTX homologues with known amino acid sequence contain His-4, the effect of His-4 on the structure and function of CTX molecules is important and is discussed in terms of the diverse membrane targets of CTX subtypes. Also discussed is the pH-induced activation of snake venom proteins in the victim.

Cardiotoxins (CTXs)[1] from cobra snake venoms are basic β-sheet polypeptides containing 60−62 amino acid residues [see Chien et al. (1994) and Dufton and Hider (1991) for the classification and list of CTX sequences]. Although the mode of action responsible for the cytotoxicity in general, and the depolarization of muscle cell and cardiomyocytes in particular (Harvey 1985, 1991), remains largely unknown, it has generally been agreed upon that a continuous hydrophobic patch flanked with positively charged lysine residues is involved in its interactions with phospholipid membranes. This requirement is evident from structure−function analysis of the interactions of CTXs with zwitterionic phospholipid dispersions (Chien et al., 1994) and the reduced hemolytic and cytotoxic activity of CTX with chemically modified lysine or aromatic residues (Kini & Evans 1989; Gatineau et al., 1990; Ménez et al., 1990; Gilquin et al., 1993; Roumestand et al., 1994).

Existing evidence points to the involvement of several different targets in the action of CTX on cell membranes. But it has been difficult to identify targets other than membrane phospholipids. In fact, a comparative study of the activity and structure relationship of 10 CTX homologues has revealed the presence of two distinct types of CTX, i.e., P-type and S-type with Pro-31 and Ser-29, respectively (Chien et al., 1994). The classification of CTXs into these two subtypes has indeed improved the previously difficult correlation of depolarization and hemolysis activities of CTXs. Furthermore, this classification suggests that diverse membrane targets may be present for different CTX subtypes. For instance, preliminary electrophysiological studies on bullfrog atrial myocytes suggest that CTX can block the inwardly rectifying background K^+ channel and concomitantly induce the formation of a novel outwardly rectifying nonspecific ion conductive pathway, I_{ctx} (Wu et al., 1993).

In a continued effort to understand the structure and activity relationship of CTX molecules, we investigated the phospholipid-related activities, i.e., membrane binding and aggregation/fusion of phospholipid vesicles, and conformational change of CTX molecule as a function of acidic pH. We chose CTX V from Taiwan cobra (*Naja naja atra*) venom (CTX A5) to illustrate these effects because a titratable amino acid residue near the physiological pH, i.e.,

† This work was supported by National Science Council, Taiwan (Grant Numbers NSC 83-0208-M007-086, 84-2113-M007-015, and 85-2113-M007-035Y).

⊗ Abstract published in *Advance ACS Abstracts,* June 15, 1996.

[1] Abbreviations: CTXs, cardiotoxins; POPC, 1-palmitoyl-2-oleoyl-*sn*-glycero-3-phosphocholine; MMPC, monomyristoyl phosphatidylcholine; Tris, tris(hydroxymethyl)aminomethane; CD, circular dichroism; NMR, nuclear magnetic resonance; 1D, one-dimension; 2D, two-dimension; NOE, nuclear Overhauser effect; TOCSY, total correlation spectroscopy; NOESY, nuclear Overhauser effect spectroscopy; Z_p, effective charge; K_p, partition constant.

S0006-2960(95)02823-6 CCC: $12.00

His-4, is present in proximity to the lipid binding site. Since 19 out of 44 CTX molecules with known amino acid sequence possess His-4, designated here as H-type CTX, the present study would shed light on the role of His-4 in CTX molecules. It should be pointed out that several additional CTX isoforms have been identified recently in Taiwan cobra venom (Chiou et al., 1995). CTX A5 is the only Taiwan cobra CTX isomer that contains histidine. Its amino acid sequence is the same as the newly corrected amino acid sequence of CLBP identified earlier by Hayashi and coworkers (Takechi et al., 1985; Chien et al., 1994).

The result of our study indicates that protonation of His-4 induces a local conformational change in CTX molecule around His-4. The pH-induced change in the lipid binding ability of CTX, however, was not due to the detected conformational change. Gouy−Chapman analysis of the binding data suggests that change in the effective charge content of CTX molecule at the membrane/water interface can provide a simple interpretation for the pH-dependent association of CTX with phospholipid membranes. There is an additional local conformational change of CTX A5 molecule around pH 5. The latter conformational change, however, completely inactivates the CTX-induced aggregation/fusion of phospholipid vesicles.

MATERIALS AND METHODS

Purification of CTXs. CTX A5 from *N. n. atra* snake venom (Sigma Chemical Company, St. Louis, MO) was purified by SP-Sephadex C-25 ion exchange column chromatography as described previously (Chien et al., 1994). The purity of CTX preparations as checked by SDS−polyacrylamide gel electrophoresis and analytical reverse phase high-performance liquid chromatography was found to be higher than 99%.

Phospholipid Monolayer. Monolayer experiments were done on a Langmuir minitrough (Joyce-Laebl Ltd.) with a home-built Teflon trough (11 cm × 17 cm × 2.5 cm, $L \times W \times H$). Data were collected by a personal computer directly connected to the experimental setup. Lyophilized POPC (1-palmitoyl-2-oleoyl-*sn*-glycero-3-phosphocholine, from Avanti Polar Lipids Inc., Alabaster, AL) was first dissolved in chloroform to a concentration of 4 mg/mL. It was then gently deposited at the air−water interface in the trough with a microsyringe in order to obtain a lipid monolayer. The starting area of the monolayer was controlled at about 600 cm^2. The surface pressure was measured by the Wilhelmy plate method using plates cut from filter paper (Whatman, No. 1).

The binding of CTX to the monolayer was studied at a constant lateral pressure of 18 mN/m and was evaluated from the increase in the area of the monolayer due to penetration of CTX into the lipid monolayer. It should be noted that the binding ability of CTX decreases at higher lateral pressure. The lateral pressure of 18 mN/m was chosen to yield a reliable change of the surface area. Since the binding of CTX to phospholipid monolayer requires hours to reach equilibrium, we used 10 mM Tris [tris(hydroxymethyl)-aminomethane]-acetate as buffer solution to avoid possible variation of the pH during the course of pH titration experiment. For ionic strength dependent experiments, the buffer with or without 100 mM NaCl was used. Therefore, 0.11 M NaCl ionic strength indicates 10 mM Tris-acetate plus 100 mM NaCl. The temperature was maintained at 25 °C.

Determination of the Effective Charge (Z_p) and Partition Constant (K_p). The association of CTX with phospholipid monolayer can be described by a simple model incorporating a water−membrane partition equilibrium modulated by electrostatic charge of the (neutral) membrane, as the basic CTX accumulates at the interface (Stankowski & Schwarz, 1990). The surface charge density of associated CTX, σ, can be calculated according to eq 1 (McLaughlin, 1977; Kuchinka & Seelig, 1989; Cevc, 1989):

$$\sigma = (Z_p e_o X_b/A_L)/[1 + X_b(A_p/A_L)] \quad (1)$$

where Z_p is the effective charge of a CTX molecule at the interface, in units of elementary charge, e_o; A_p is the surface area occupied by a protein molecule; A_L is the surface area occupied by a lipid molecule; and X_b is the mole fraction of CTX partitioned in lipid monolayer.

The concentration of CTX, C_{ctx}, at the plane of CTX binding immediately adjacent to the membrane surface was calculated from the concentration of CTX in the bulk, C_{eq}, according to Boltzmann equation:

$$C_{ctx} = C_{eq} \exp(-Z_p \psi_o F_o/RT) \quad (2)$$

and the partition equilibrium was calculated by the following relation:

$$K_p = X_b/C_{ctx} \quad (3)$$

The surface potential, ψ_o, which is generated by the surface charge density, was calculated using the Gouy−Chapman theory:

$$\sigma^2 = 2000\epsilon_o\epsilon_r RT\sum C_{i,eq}[\exp(-Z_{io}\psi_o F_o/RT)^{-1}] \quad (4)$$

where $\epsilon_r = 78$ is the dielectric constant of water, ϵ_o the permittivity of free space, R the gas constant, $C_{i,eq}$ the concentration of the ith electrolyte in the bulk aqueous phase, and Z_i the charge of the ith species.

The surface area of POPC was estimated from monolayer measurements as $A_L = 70$ Å^2 at 18 mN/m (Evans et al., 1987). The increase in membrane surface area upon CTX binding was estimated to be about 400 Å^2 on the basis of the molecular structural information of CTX A5 by assuming that the three-finger loops are involved in the CTX−membrane interaction (Chien et al., 1994). This assumption is consistent with the NMR result reported recently for binding CTX toxin γ to phospholipid micelles (Dauplais et al., 1995). It should be pointed out that the exact magnitude of surface area does not affect our major conclusion on the important role of effective charge in monitoring the pH-dependent binding, since essentially the same surface area and partition constant were used to generate theoretical curves for data obtained under different pH and ionic strength (see Results). Furthermore, the results can be reasonably described using Gouy−Chapman analysis by assuming the constancy of the interaction of CTX with phospholipid membranes.

Aggregation/Fusion Assay. Small unilamellar sphingomyelin vesicles were prepared by ultrasonication, and the apparent aggregation/fusion activity assay was performed at the sphingomyelin transition temperature (42.5 °C) as

described before (Chien et al., 1991, 1994). Experiments were done with 200 μM vesicles, 2.0 or 0.7 μM CTX A5, in solution containing 10 mM Tris-acetate and 100 mM NaCl at the indicated pH.

Proton NMR Spectroscopy. One-dimensional ^{1}H NMR spectra were recorded at 25 °C on either a Bruker MSL-300 or a DMX-600 spectrometer. A known amount of CTX A5 (about 5−7 mg) was first dissolved in 0.5 mL D_2O containing the desired salt or buffer solution with or without 60 mM MMPC (monomyristoyl phosphatidylcholine, Avanti). 2 N HCl was then used to titrate the sample, and the pH was recorded by a 3 mm glass electrode right before and after the spectra were recorded. The heavy atom effect was found to be about 0.1 pH unit as judged by the apparent pK_a values of His-4 determined in 10% or 99.9% D_2O. The effect of different buffer solutions, as demonstrated in the Result, was found to be negligible.

For ^{1}H two-dimensional (2D) NMR experiments, data were acquired at 25 °C on a Bruker DMX 600 spectrometer. TOCSY (Bax & Davis, 1985) and NOESY (Jeener et al., 1979; Macura & Ernest, 1980; Anil-Kumar et al., 1980) 2D NMR spectra were obtained with 4 mM CTX A5 in H_2O/D_2O (90/10, v/v) at four different pH, i.e., pH 2.5, 3.5, 5.1, and 7.0. Before the desired pH was reached, a stepwise pH titration of the sample was carried out to obtain a series of 1D ^{1}H NMR spectra at the reported pH values. TOCSY with a mixing time 55 ms and NOESY with a mixing time 100 and 250 ms were recorded in the phase-sensitive mode using time-proportional phase incrementation (Marion & Wüthrich, 1983). Suppression of water signal was achieved by pulsed field gradient (Piotto et al., 1992). 2D spectra were acquired with 512 × 2048 data points and with a spectral width of 7184 Hz and were processed by *uxnmr* (Bruker). Chemical shifts are reported relative to HOD at 4.8 ppm.

CD (Circular Dichroism) Measurement. For pH titration experiments, CD spectra were recorded at 25 °C on an AVIV 62A DS spectropolarimeter (Lakewood, NJ), using 1 mm path length cells with a time constant of 1 s, and a bandwidth of 1 nm. Samples of 20 μM CTX A5 in H_2O with or without 0.6 mM MMPC were used. The spectra were the average of eight repeats. Data are reported as mean residue ellipticity.

Determination of Apparent pK_a. Unless mentioned otherwise, the apparent pK_a values for pH-dependent ^{1}H NMR chemical shifts were obtained by nonlinear least-squares fitting of the observed parameters to Hill equation of the one-proton titration curve:

$$\delta_{obs} = \delta_x + \Delta\delta K_a/([H^+] + K_a) \quad (5)$$

where δ_{obs} is the observed parameter, δ_x is the parameter at protonated state, $\Delta\delta$ is the parameter difference between protonated and deprotonated states, K_a is the association constant, and $[H^+]$ is the concentration of protons in solution.

RESULTS

Binding of CTX to Phosphatidylcholine Monolayers

pH-Dependence. As shown in the representative trace of binding of CTX A5 to POPC monolayer (Figure 1A), the membrane surface area increases instantaneously upon addition of CTX A5, at pH 7.0. This increase reached a plateau within 2 h in our monolayer setup. The percentage increment

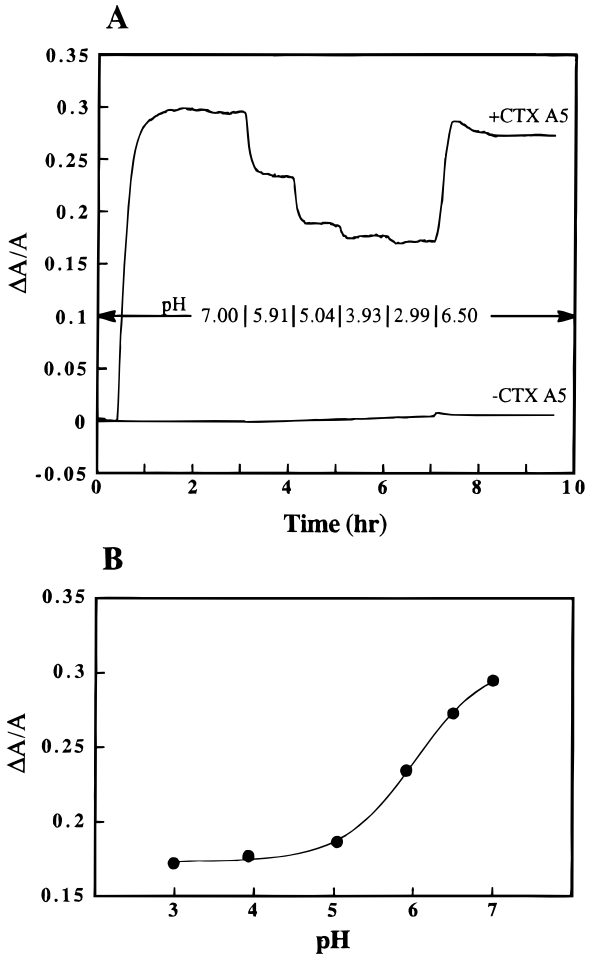

FIGURE 1: Representative traces of binding of CTX A5 to POPC monolayers at indicated pH (A) and the pH-dependent association of CTX A5 with monolayer membranes (B). Traces shown in panel A were obtained in the presence (+ CTX A5) or absence (− CTX A5) of 50 nM CTX A5 in 10 mM Tris-acetate and 100 mM NaCl. The simulated curve shown in panel B indicates an apparent pK_a value of 6.0 for the pH-dependent association of CTX A5 with POPC monolayer.

of the surface area, i.e., $\Delta A/A$, was found to decrease upon titrating with 4 N HCl to reach the desired pH. For instance, by decreasing the pH from 7.0 to 5.9, $\Delta A/A$ was found to decrease from about 30% to 23%. This decrease in $\Delta A/A$ was, however, smaller at lower pH. As can be seen in the figure, the difference in $\Delta A/A$ values between pH 5.0 and 3.9 is less than 2%, which is significantly lower than that observed between pH 7.0 and 5.9.

This process was reversed upon titrating from pH 2.99 back to pH 6.5, as judged by the increase of $\Delta A/A$. This suggests that POPC monolayer maintains a constant state under the experimental condition of high ionic strength during the experimental time span of several hours and is suitable for CTX binding study. Control experiment in the absence of CTX A5 lends support to this conclusion (see bottom trace shown in Figure 1A).

The pH-dependent change in surface area implies binding process with an apparent pK_a value of about 6.0 (Figure 1B). This suggests that probably histidine affects the CTX−phospholipid interaction. ^{1}H NMR experiments that allowed the assignment of specific amino acids involved in the process will be presented later.

Ionic Strength Dependence. The effect of ionic strength was studied in order to understand the role of electrostatic

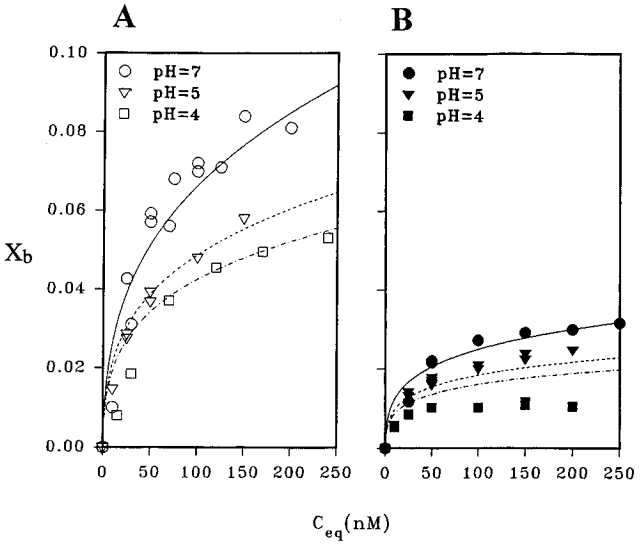

FIGURE 2: Langmuir adsorption isotherm of CTX A5 to POPC monolayer at indicated pH and ionic strengths of 0.11 M (A) and 0.01 M (B). The circles, triangles, and squares represent data points measured at pH 7.0, 5.0, and 4.0, respectively. The simulated curves are produced by assuming the same K_p value of 10^7 in both panel A and B. Effective charge values (Z_p) of 2.2, 2.6, and 2.8 are used to generate three consecutive curves from top to bottom. Please see Materials and Methods section for the details of calculation.

shielding in the binding of CTX to phospholipid membranes (compare Figure 2A with B). Qualitatively, low pH and low ionic strength were found to decrease the binding of CTX to membrane. It should be mentioned that CTX appears to destabilize POPC monolayer at low pH and low ionic strength. Instead of obtaining a plateau as shown in Figure 1A, we found that the surface area of monolayer detected at low pH and low ionic strength appeared to reach a peak followed by slow decay as a function of time upon CTX treatment (data not shown). The data obtained at pH 4 with 10 mM Tris (closed square shown in Figure 2B) were taken from the peak value. These values may have been underestimated since decay of the surface area may have already occurred right after CTX treatment.

Above all, both the ionic strength and pH-dependence of the association of CTX with phospholipid monolayer indicate that electrostatic potential near the membrane surface is definitely involved in this interaction. Low ionic strength and low pH are expected to increase the magnitude of electrostatic force by increasing the Debye shielding length and positive charge content, respectively, of CTX at the water−membrane interface. Quantitative analysis of the data was then performed according to Gouy−Chapman equation (see Materials and Methods). The six simulated curves shown in Figure 2 represent the results of such calculation using the parameters shown in the figure legend.

It should be pointed out that all six curves were generated using the same parameter with effective charge as the only variable. The data of best fit indicate that the effective charge of CTX near the membrane surface increases from 2.2 to 2.6 when the pH decreases from 7.0 to 5.0, assuming the increase in membrane surface area upon CTX binding to be about 400 Å^2 per CTX A5 molecule. Slightly higher values of 2.6 and 3.1, respectively, were obtained for the effective charge of CTX when a larger increase in membrane surface area of 600 Å^2 per CTX A5 molecule was assumed. These experimentally determined values of effective charge, however, are much smaller than would be estimated from the total charge content of CTX molecule or from the titratable amino acid residues in the pH range studied. The implication of this observation will be discussed later.

Significant deviation between the simulated curve and the experimental data was found for experiments carried out at pH 4.0 with 10 mM ionic strength (Figure 2B). But, as pointed out earlier, the monolayer does not appear to be stable under this experimental condition. Therefore, the ionic strength and pH-dependence of the association of CTX with membrane can largely be taken to be a result of electrostatic interaction at the membrane−water interface.

The initial slope of the binding isotherm represents the partition coefficient of CTX−membrane interactions (Stankowski & Schwarz, 1990). As shown in Figure 2A, a significant deviation in the values measured from simulated curves can indeed be observed at concentrations lower than 50 nM. This suggests that the binding of CTX to the membrane, in addition to simple electrostatic interaction near the membrane surface, was also perturbed by pH titration. The possible error of the data precludes the quantitative determination of the respective partition coefficient at pH studied. Nevertheless, the effect is found to be small and the estimated partition coefficient, in the studied pH range, can be considered to be of the same order of magnitude.

pH-Dependence of Local Conformational Change of CTX

Proton NMR Study at 300 MHz. In order to identify the molecular origin of the pH-dependent CTX association with membranes, ^{1}H NMR spectroscopy was applied to study the interaction of CTX A5 with phospholipid micelles. Our first approach was simply to follow the chemical shift of the identifiable resonances from CTX as a function of pH in the presence and absence of MMPC micelles (Figure 3). It is well-known that the ^{1}H NMR signals located in the ring-current shift region between 6 and 8 ppm arise mainly from the side chains of His, Tyr, and Phe. CTX A5 contains one His, two Tyr, and four Phe amino acid residues with assignable ^{1}H NMR signals, and these would serve as a guideline to follow the conformational change of CTX.

As shown in Figure 3A and C, the C2 proton peak of His-4 of lipid-free CTX A5 detected in the chemical shift range between 8 and 9 ppm at 300 MHz NMR was found to vary as a function of pH* with an intrinsic pK_a value of 5.6. [We use pH* to represent the uncorrected pH value for CTX in 99% D_2O solution used in the one-dimensional ^{1}H NMR study, and the nomenclature of atoms in imidazole ring is from Wüthrich (1986).] The effect of different buffer solutions on the pK_a value appears to be negligible since the measured chemical shifts were found to be the same for CTX in 100 mM NaCl or in 100 mM KCl with 100 mM phosphate buffer (compare the open symbols with the closed symbols shown in Figure 3C). In addition, the heavy atom effect of D_2O was found to be small. The pK_a value of His-4 for CTX in 10% D_2O (without salt) was found to be around 5.5 (Figure 6A), about 0.1 pH unit lower than CTX in 99.9% D_2O. Interestingly, the signal due to the side chain of Tyr-12 at 6.8 ppm also varies as a function of pH* with similar pK_a value of 5.6. Since, unlike His, there is no titratable group for Tyr within the pH range studied, the detected chemical shift change can be attributed either to the direct pH-induced conformational change in the loop I region or

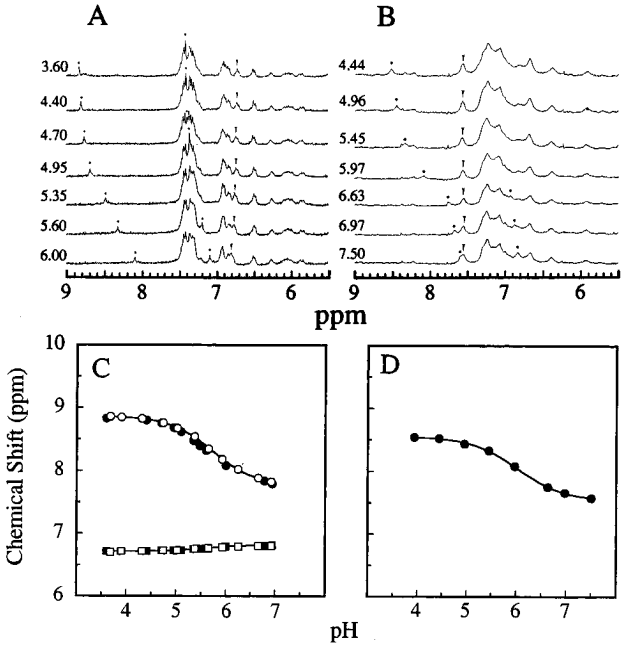

FIGURE 3: Proton NMR studies to determine the pK_a values of titratable histidine of CTX A5 in the absence (panels A and C) and presence (panels B and D) of MMPC micelles. Proton 300 MHz NMR spectra were obtained at 25 °C in 99% D_2O. The circles shown in panels C and D represent pH-dependence of ^{1}H NMR chemical shift of His-4 C_2 proton, whereas the squares shown in panel C represent pH-dependence of ^{1}H NMR chemical shift from $C_{3,5}$ protons of Tyr-12. The open symbols represent data obtained with 100 mM NaCl D_2O solution, and the closed symbols represent, data obtained with 100 mM KCl and 100 mM phosphate D_2O solution. The desired pH values were obtained by titrating with NaOD. The solid lines are the best-fit curves for the determination of pK_a values of the pH-dependent chemical shifts.

to the secondary ring-current shift effect due to the protonation of the imidazole ring of His-4. Additional experiments to indicate the presence of pH-induced conformational change need to be performed by 600 MHz NMR.

The use of ^{1}H NMR to study the conformational change of CTX in the presence of lipid is more difficult because the line width becomes broader upon addition of MMPC micelles (Figure 3B). For instance, the Tyr-12 resonance at around 6.8 ppm was observable only for pH higher than 6.6. Nevertheless, the C2 proton peak of His-4 in CTX/MMPC complex is still well-resolved. Its pK_a value can then be determined to be around 6.0 (Figure 3D), about 0.4 pH* units higher than that determined in the absence of MMPC. We have previously shown that the pH-dependent association of CTX with membranes exhibits a best-fit pK_a value of about 6.0. It can be concluded that the protonation/deprotonation process of His-4 is mainly responsible for the pH-dependent binding ability of CTX to membranes.

There are several unassignable signals in the 300 MHz NMR spectra of CTX/MMPC micelles. For instance, a new peak around 7.55 ppm, emphasized by the arrow shown in Figure 3B, is clearly visible. A lipid-induced local conformational change may occur at least for the amino acids with aromatic side chains. The higher pK_a value for CTX in lipid micellar dispersions as compared to free CTX molecule is also consistent with this interpretation. It should be emphasized that the β-sheet structure of CTX and the four disulfide bonds of this molecule are intact under this experimental condition. Recent high-field 2D NMR study of the interaction of toxin γ from *Naja nigricollis* with perdeuterated dodecyl PC has also suggested that the micellar environment only induces stabilization of the triple-stranded β-sheet without significant change in the overall three-dimensional structure of CTX molecule (Dauplais et al., 1995). Therefore, the conformational change detected reflects only a conformational change in a local region.

Proton NMR Study at 600 MHz. In view of the local conformational change suggested by low-field ^{1}H NMR study, 2D ^{1}H NMR study was carried out at 600 MHz to investigate the extent of the local conformational change induced by the protonation of His-4 residue. As shown in Figure 4, the characteristic main-chain β-sheet NOE (nuclear Overhauser effect) connectivities determined by 2D NMR were found to be the same for CTX A5 studied at pH 5.1 and 7.0. For instance, the NOE connectivities of the amide protons for the amino acid residues in both double-stranded antiparallel β-sheet (loop I region) and triple-stranded antiparallel β-sheet (loop II and III region) remain the same between pH 5.1 and 7.0. In addition, the residues 18−21 and 58−61 show patterns of NOE connectivities characteristic of a type II turn (Wüthrich, 1986). Similarly, residues 48−51 form a type I turn in the pH range studied. Other long-range NOE connectivities (H_α/Thr-26 to H_N/Val-36, H_N/Leu-27 to H_N/Val-36, H_N/Val-36 to H_N/Lys-37, and H_N/Leu-27 to H_α/Pro-35) to indicate the presence of β-bulge in the middle of loop II are also detected (Gilquin et al., 1993). Therefore, the overall three-dimensional structure of CTX A5 can be considered to be insensitive to the protonation and deprotonation of the imidazole ring of His-4.

However, there is evidence to suggest that the local conformation near His-4 undergoes subtle changes. For instance, NOESY spectra obtained at pH 7.0 show that the amide proton of His-4 interacts with its C2 proton, but this NOE connectivity disappears at pH 5.1. This suggests that the imidazole ring of His-4 indeed undergoes reorientation during the protonation process. In addition, the C_α proton of Phe-23 also interacts with amide proton of Cys-55 at pH 7.0, whereas this NOE connectivity disappears at pH 5.1. This suggests that local conformational change also occurs in the triple-stranded β-sheet region due to the protonation of His-4 side chain. These effects, although considered to be too small to affect the overall three-dimensional structure of CTX, can be important in the stability of CTX molecule. Recent NMR study of the chemically modified toxin γ has suggested a possible correlation between the structural stability and toxicity of CTXs (Roumestand et al., 1994). In the following section, the extent of the structural perturbation induced by pH is described using the pH-dependent chemical shift variation which is known to be more sensitive to local conformational change in proteins (Pardi et al., 1983).

Figure 5 shows the TOCSY spectra obtained at pH 7.0 (panel A) and 5.1 (panel B). The chemical shifts of amide protons from His-4, Asn-5, Phe-10, Ile-11 and Tyr-12, emphasized by the arrows shown in Figure 5, are found to shift significantly between the two pH ranges. The chemical shift of the amide proton of His-4, for example, was found to be about 9.38 and 9.65 ppm at pH 7.0 and 5.1, respectively (see the cross-peak at extreme left emphasized by the arrow). The titration curve of this proton obtained by 1D NMR study shows a pH-dependence and a pK_a value of about 5.5 (Figure 6A). The fact that a similar pK_a value has been detected using NMR signals from the imidazole ring of His-4 and the side chain of Tyr-12 (Figure 3C) clearly indicates that

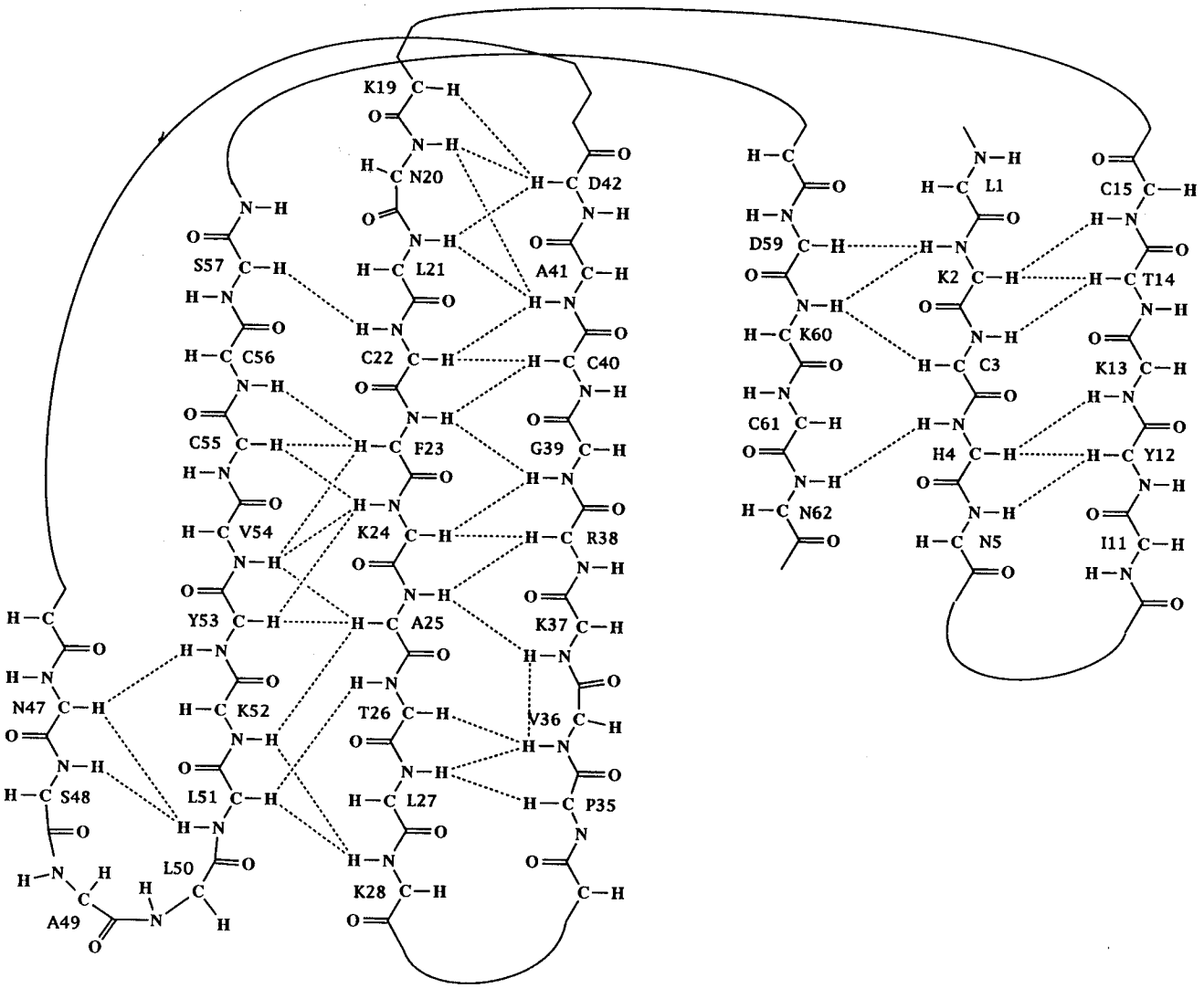

FIGURE 4: Schematic diagram to indicate NOE connectivity of the amide protons in the double-stranded antiparallel and triple-stranded antiparallel β-sheet of CTX A5 as determined by 2D NMR at pH 5.1 and 7.0. The same diagram was obtained for CTX A5 regardless of the protonation or deprotonated state of His-4.

the amide proton can also sense the protonation and deprotonation processes of the imidazole ring of His-4 amino acid side chain.

All of the pH-dependent resonances shown in Figure 6, including amide protons from several amino acid residues including Ala-41, Cys-22, Lys-24, and Ala-25 outside the loop I region, can be described reasonably by a single pK_a of about 5.5. These changes can only result from a direct effect of the locally perturbed conformation since all of the aforementioned amide protons are located far away from the imidazole ring of His-4 (Figure 7). For example, the amide proton of Ala-41 is 13.6 Å away from the imidazole ring as estimated from the three-dimensional NMR structure of CTX A5 determined at pH 3.7.

As summarized in Figures 7 and 8A, various amide proton NMR signals are influenced by the protonation of the imidazole ring of His-4. It can be seen that the amide protons of Lys-60, Cys-61, and Asn-62 in the C-terminal (see the 2D spectra shown in Figure 5) also shift significantly. The pH-induced structural perturbation in the C-terminal region, detected in both NOE connectivities and chemical shift variations, is not surprising in view of its proximity to His-4. The perturbation in the triple-stranded antiparallel β-sheet (Cys-22, Lys-24, Ala-25, and Ala-41) region probably can also be understood since Cys-22 is covalently linked to Cys-3 via disulfide bond.

There is also marked chemical shift variation for the amide protons of Lys-33 and Arg-38. The effect detected in Lys-33 is most interesting despite the relatively small difference in its amide proton detected between pH 5 and 7. The amide proton of Lys-33 is far from His-4 as detected by solution NMR structure determined at pH 3.7. However, the X-ray crystal structure of CTX A5 determined at pH 8.5 reveals that the tips of loop I and II are much closer due to the "water-binding" ability of loop II in P-type CTX molecules (Bilwes et al., 1994; Sun et al., 1996).

Included in Figure 8 is a comparison of the chemical shift differences of amide protons between pH 5.1 and 3.5 (panel B) and between pH 3.5 and 2.5 (panel C). The result suggests that most of the chemical shift differences detected at different pH are due to the protonation/deprotonation of other titratable groups such as Glu-17 (panel B) and Asp-42 (panel C). A detailed study on the role of these acidic amino acid residues in the structural stability of CTX molecules will be presented elsewhere (Chiang et al., 1996). The pK_a of side-chain carboxylate groups of Glu-17 and Asp-42 can simply be judged to be in the range of pH 4 (between pH 5.1 and 3.5) and 3 (between pH 3.5 and 2.5), respectively.

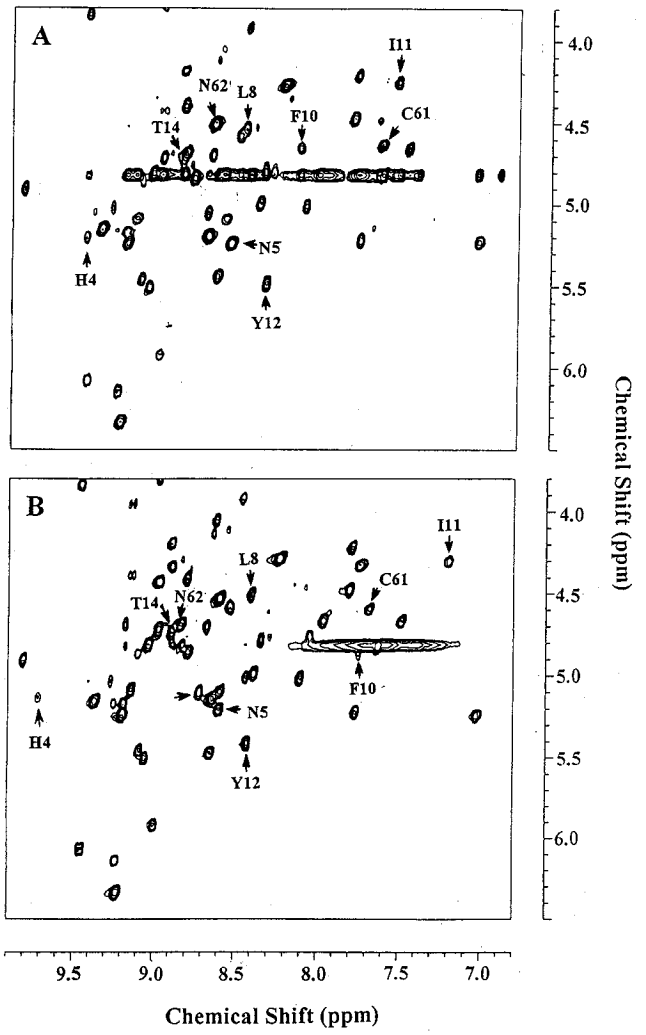

FIGURE 5: Fingerprint regions of the TOCSY 2D NMR spectra (600 MHz, 55 ms mixing time) of CTX A5 in 10% D_2O at 25 °C: pH 7.0 (A) and pH 5.1 (B). The arrows indicate cross peaks with significant variation of the chemical shift.

It should be pointed out that the protonation of each acidic side chain may span three pH units. Therefore, chemical shift differences determined at two pH, e.g., between pH 5.1 and 3.5 (panel B), may reflect the combined effect of protonation of amino acid side chains of His-4, Glu-17, and Asp-42. As we will show later, a conformational change in CTX A5 due to the combined effect of these amino acid residues can indeed be detected, by CD spectroscopy, between pH 4 and 6.

Circular Dichroism Study. As shown in Figure 9, there is a detectable pH-induced conformational change in CTX A5 as measured by CD. This is clearly evident by the higher ellipticity at 205 nm for the measurement carried out at lower pH. In fact, the CD ellipticity detected at 205 nm changes from about 0.3×10^3 to about 2×10^3 deg cm^2/dmol, and an abrupt change occurs between pH 6 and 4. It should be pointed out that although the change is small, it is reproducible within the acceptable pH variation range. The effect is probably due to the cooperative process involving the protonations of side chains of Glu-17 and His-4 (Figure 8B). Qualitatively similar results can also be observed if the CD intensity at 195 nm is used to follow pH-dependent conformational change (data not shown). This suggests that conformational changes detected by CD may be a result of pH-dependent processes occurring in different regions of the

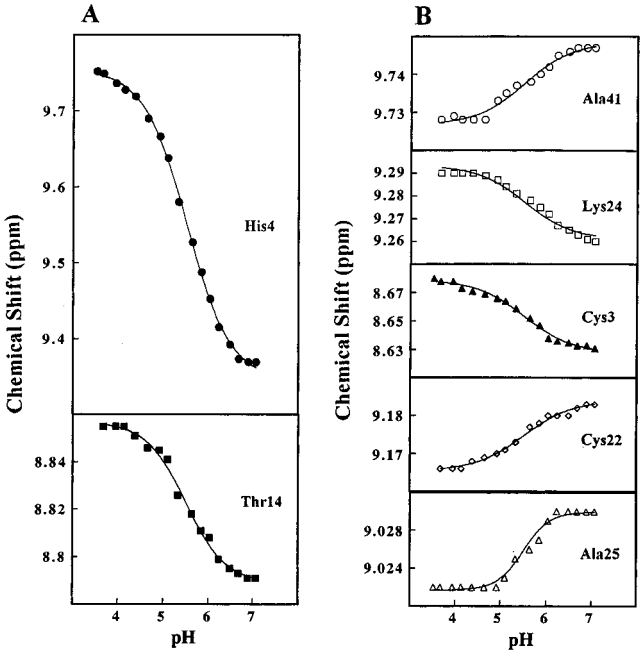

FIGURE 6: pH-dependence of the ^{1}H NMR chemical shift of NH protons of the amino acid residues exhibiting an apparent pK_a values similar to His-4. The curve shown for His-4 was the least-squares fit of the data obtained by 1D ^{1}H NMR (600 MHz) spectra of CTX A5 at indicated pH, whereas other curves were generated using a fixed pK_a value of 5.5. As seen all of the data can be described reasonably by the same pK_a value.

molecule. Nevertheless, the result obtained by CD study is consistent with that obtained by NMR and suggests that an additional conformational change occurs between pH 4 and 6.

Lipid-induced conformational changes corresponding to an increase in the content of a β-sheet at the expense of the nonordered conformation have previously been suggested on the basis of IR, CD, and NMR measurements (Surewicz et al., 1988; Chien et al., 1994; Dauplais et al., 1995). Consistent with the previous reports, an additional conformational change in the presence of MMPC micelles occurs and causes an additional increase in ellipticity at 205 nm (upper trace in Figure 9). It should be emphasized here that more than one process may be responsible for the detected change in the CD spectra: one due to the pH effect, the other due to the lipid effect. Therefore, the relative change in the presence and absence of lipid micelles as detected by CD measurements can only be considered to be qualitative.

pH-Dependence of CTX-Induced Aggregation/Fusion of Sphingomyelin Vesicles. We have previously shown that CTX A5 induces apparent aggregation/fusion activity of sphingomyelin vesicles (Chien et al., 1991). CTX-induced fusion of phospholipid vesicles is sensitive to the transition temperatures of the studied phospholipid membranes regardless of the phospholipid used. Sphingomyelin, however, is advantageous over phosphatidylcholine in that the complication arising due to possible residual phospholipase A_2 contamination can be overcome (Chien et al., 1994). Figure 10A and B show the turbidity change of sphingomyelin vesicles induced by CTX at 42.5 °C as a function of time at the indicated pH. It is emphasized again that the present assay is quite sensitive to the transition temperature of phospholipid vesicles, and therefore, the absolute turbidity values measured may vary significantly depending on the

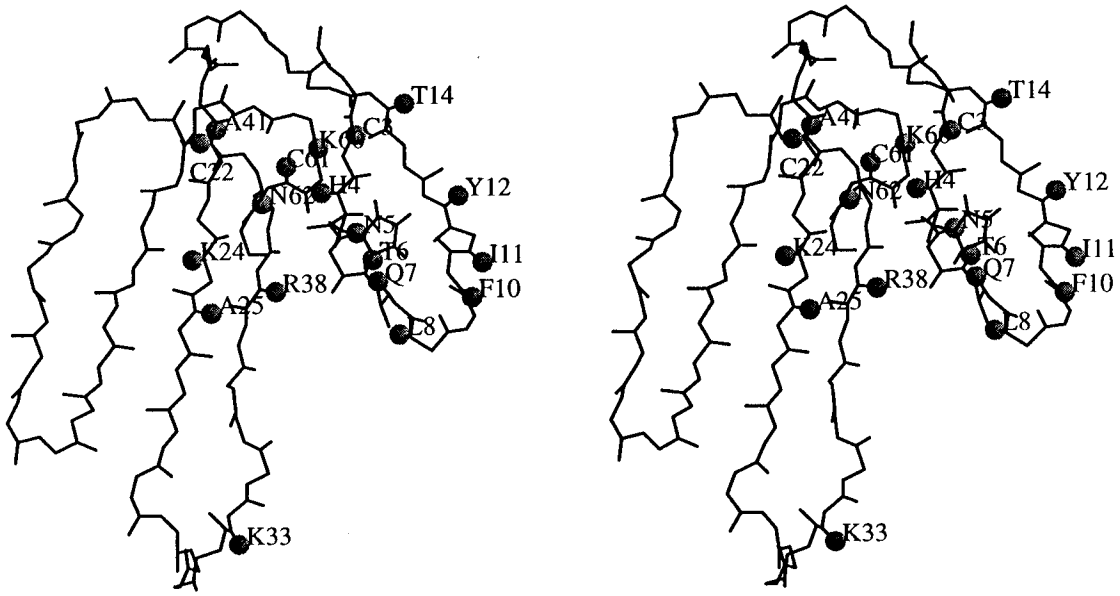

FIGURE 7: Stereoview of the structure of CTX A5 showing the backbone atoms with dark circles to indicate the NH protons of the residues where a pH-dependent chemical shift variation was observed due to the protonation of the imidazole ring in His-4 amino acid residue. The values of H_N chemical shift variation can be found in Figure 8A.

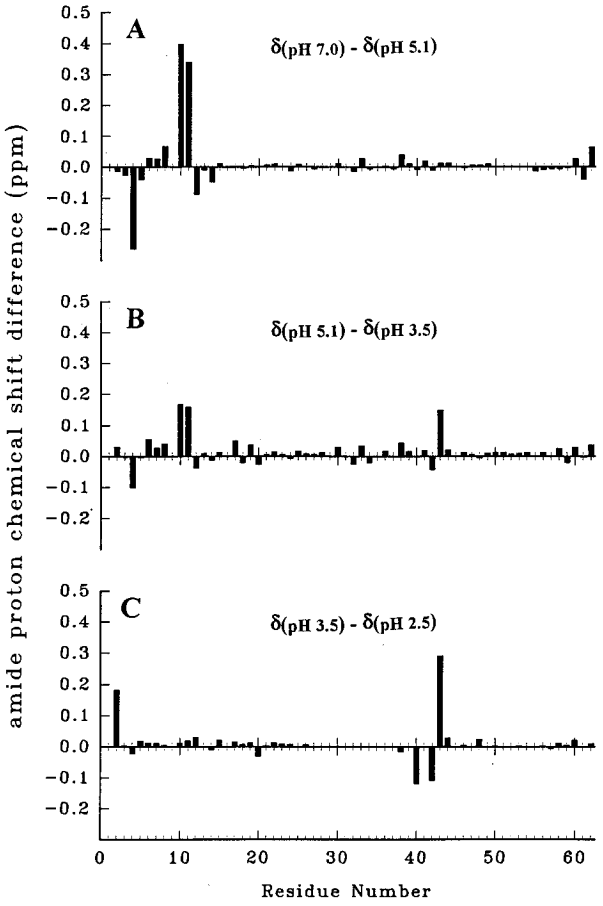

FIGURE 8: Comparative studies of the ^{1}H NMR chemical shifts of NH amide protons at the indicated pH. Chemical shift differences between pH 7.0 and 5.1 (A), pH 5.1 and 3.5 (B), and pH 3.5 and 2.5 (C) are shown.

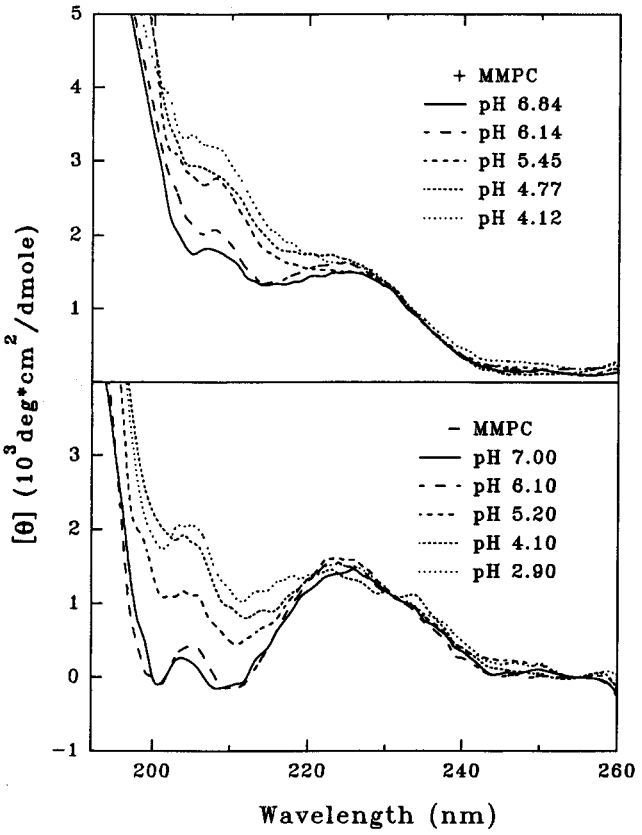

FIGURE 9: CD spectroscopic study of pH-induced conformational change of CTX A5 in the presence (upper traces) and absence (lower traces) of MMPC micelles. Note the abrupt change of the CD spectra 205 nm around pH 5.

sample preparation and the variation in the temperature control. Nevertheless, low pH was always found to inhibit the activity.

Shown in Figure 10C is the pH-dependence of aggregation/fusion activities as measured by the turbidity change of phospholipid vesicles at two different concentrations of CTX. Apparently, the activity is saturated at pH value higher than 5 for samples with a high CTX/phospholipid ratio. In contrast, there is no detectable activity at below pH 3. It should be noted that only about 50% of CTX was released from phospholipid monolayers by lowering pH from 7 to 3 (Figure 2). In addition, sphingomyelin vesicles remained intact even at a lower pH value of 3 within the experimental time span of several hours. The lower activity could

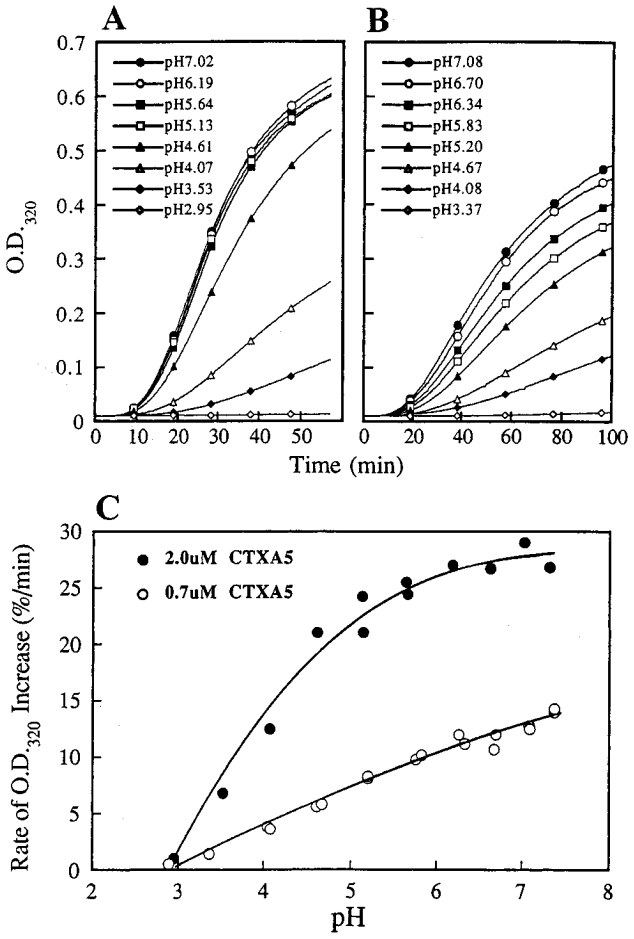

FIGURE 10: Effects of pH on the CTX-induced aggregation/fusion activity of sphingomyelin vesicles as studied by the turbidity change at 320 nm: change in the optical density of 200 μM sphingomyelin vesicles, induced by (A) 2.0 μM and (B) 0.7 μM CTX, at the indicated pH values. (C) pH-dependence of the CTX-induced aggregation/fusion activity of sphingomyelin vesicles as determined by the initial rate of the turbidity change as a function of time (Chien et al., 1991).

therefore be attributed to the conformational change of CTX at pH around 5.

DISCUSSION

This is the first report showing that the phospholipid-related activities of snake cardiotoxin CTX A5, measured by the increase in the surface area of Langmuir monolayer membrane and the apparent CTX-induced aggregation/fusion of sphingomyelin vesicles, are significantly inactivated at low pH. On the basis of Gouy−Chapman analysis, the inactivation detected between pH 5 and 7 is attributed mainly, but not solely, to the change in the effective charge content of CTX molecules at the membrane−water interface as a result of protonation of His-4. On the basis of CD spectroscopic measurement, the inactivation detected around pH 5 is attributed mainly to conformational change in the CTX A5 molecule. The results suggest that deciphering the functional sites of CTXs on the basis of structure and dynamics determined at low pH should be done with caution.

The protonation and deprotonation of the imidazole ring of His-4 also induce conformational change in several regions, notably in loop I, the C-terminal, and the triple-stranded antiparallel β-sheet of CTX molecule, although the characteristic hydrogen bonding pattern of all the β-sheets in the CTX molecule remains largely unperturbed. Both CD and NMR data support this conclusion. Since the imidazole side chain of His-4 is aligned toward the C_α proton of Phe-10 at pH 3.7 (Singhal et al., 1993), most of the chemical shift variations observed for the amino acid residues located in the loop I region can be explained if the imidazole ring of His-4 is assumed to reorient at high pH. The chemical shift variations observed in the C-terminal and triple-stranded antiparallel β-sheet region should reflect the locally perturbed structure/dynamics of CTX molecule. The effect of His-4 protonation on the triple-stranded β-sheet region is most interesting because it indicates that local conformational change can propagate to distant regions via the disulfide bond.

We discuss below the implication of the effective charge content, Z_p, determined in binding of CTX to membrane surface. It is suggested that Z_p, determined by Gouy−Chapman analysis, may provide a useful constraint on the binding state of CTX molecules at the membrane interface. Finally, the biological significance of H-type CTX molecules is discussed in terms of diverse targets of CTXs in biological membranes and the pH-dependent activation of snake toxins at physiological pH.

Geometric Constraint Provided by Z_p. At neutral pH, the effective charge of the CTX molecule near the POPC membrane surface is found to be about 2.2, assuming the increase in membrane surface area upon CTX binding to be about 400 Å^2 per CTX A5 molecule. CTX A5 is a basic polypeptide containing 11 Lys, one Arg, one His, one Glu, and two Asp amino acid residues. Thus, the effective charge determined according to the simple Gouy−Chapman model is about 3−4 folds lower than the theoretical value of 9.

The effective charge of the titratable His-4 is also found to be lower than the theoretical value. Proton NMR study of CTX molecule as a function of pH indicates that the pK_a of His-4 is around 6.0 in the presence of phospholipid micelles. Based on the NMR titration curve, about 80% of His-4 was found to be protonated between pH 5 and 7 (Figure 6). Gouy−Chapman analysis of the CTX binding isotherm, however, reveals an increase of only about 0.4 charge units from pH 7.0 to 5.0 (Figure 2). Even if one assumes an increase in membrane surface area upon CTX binding to be about 600 Å^2 per CTX A5 molecule, which is an upper limit based on the molecular modeling of CTX A5, an increase of about 0.5 charge units was measurable from pH 7.0 to 5.0. Therefore, the effective charge content of His-4 has also been reduced by about 2-fold.

In the Gouy−Chapman model the surface charges are assumed to reside at the interface of the membrane. A reduction in apparent charge to an effective value is expected, since not all of the charged residues are located right at the membrane surface. It has been suggested that the localization of charges at 10 Å from the interface, about the order of one Debye length at 100 mM of univalent electrolyte, would reduce the effective potential by nearly a half with respect to that produced by charges at the interface (Ohshima & Ohki, 1985).

His-4 of CTX A5 is separated by four amino acid residues from the first hydrophobic amino acid residue, Leu-8, in the loop I region. Therefore, the distance between His-4 and Leu-8, an amino acid residue proposed to be involved in membrane binding, can be estimated to be about 12 Å, by assuming the distance translation of parallel β-sheet per

residue to be about 3.2 Å. Alternatively, the distance between the C_α of His-4 and Leu-8 calculated from the solution structure of CTX A5 is found to be about 9.6 Å. It is therefore reasonable to assume that the protonated imidazole group is about 10 Å away from the Leu-8 residue. The reduction of the effective charge from the apparent one, as in the case of His-4, can then be easily accounted for by the distance factor.

It should be pointed out that other factors such as counterion binding/screening may also significantly affect the determination of effective charge. Nevertheless, if distance is the sole factor in reducing the physical charge, the main-chain polypeptide located between the His-4 and Leu-8 amino acid residues would lie perpendicular to the membrane surface. Future theoretical and experimental investigations using site-directed mutagenesis CTX (Chi et al., 1994) may provide useful information on the binding mode of CTX to phospholipid micelles.

Diverse Targets for CTX Subtype. The pH-dependent behavior of CTX A5 may be a general property of all H-type CTXs from a structural point of view. It is not known how such a behavior can be related to any biological activity in view of the low pK_a in comparison with physiological neutral pH. However, it should be remembered that the membrane surface usually consists of many acidic groups in both inner and outer leaflets. A simple argument based on the Gouy−Chapman analysis would suggest that pH at the membrane interface is about 1 to 2 units lower than the physiological neutral pH. Therefore, one would expect that the pH-dependent behavior of H-type CTX at the biological membrane surface, e.g., local conformational change of loop I to be a result of His-4 protonation, could induce more structural fluctuation in the already flexible loop I region of CTX molecule.

The pH-dependence of the binding of CTX to phospholipid membranes provides plausible explanation for the inertness of CTX molecules within the acidic venom gland (Le Goas et al., 1992), although they exhibit cytolytic activity at physiological pH. The three-dimensional structures of α-cobratoxin and epidermal growth factor have recently been determined by NMR at acidic and physiological pH in solution (Kohda and Inagaki, 1992; Le Goas, 1992; Leroy et al., 1994). Both polypeptides exhibit pH-dependent variations in local conformation, although the overall three-dimensional structures at acidic pH are similar to those at physiological pH. Interestingly, similar to CTX, both polypeptides are inactive at low acidic pH. Therefore, it will be of future interest to investigate whether simple electrostatic interaction, in addition to the pH-induced local conformational change, also plays important role in receptor recognition of these polypeptides near the membrane surface.

ACKNOWLEDGMENT

We are indebted to the Hsinchu regional research facility center for the usage of Bruker DMX-600 NMR spectrometer.

REFERENCES

Anil-Kumar, Ernst, R. R., & Wüthrich, K. (1980) *Biochem. Biophys. Res. Commun. 95*, 1−6.

Bax, A., & Davis, D. G. (1985) *J. Magn. Reson. 65*, 393−402.

Bilwes, A., Rees, B., Moras, D., Ménez, R., & Ménez, A. (1994) *J. Mol. Biol. 239*, 122−136.

Cevc, G. (1989) *Biochim. Biophys. Acta 1031*, 311−382.

Chi, L. M., Vyas, A. A., Rule, G. S., & Wu, W. (1994) *Toxicon 32*, 1679−1683.

Chiang, C.-M., Chang, S.-L., Lin, H.-j., & Wu, W. (1996) *Biochemistry 35*, 9177−9186.

Chien, K.-Y., Huang, W.-N., Jean, J.-H., & Wu, W. (1991) *J. Biol. Chem. 266*, 3252−3259.

Chien, K.-Y., Chiang, C.-M., Hseu, Y.-C., Vyas, A. A., Rule, G. S., & Wu, W. (1994) *J. Biol. Chem. 269*, 14473−14483.

Chiou, S.-H., Hung, C.-C., Huang, H.-C., Chen, S.-T., Wang, K.-T., & Yang, C.-C. (1995) *Biochem. Biophys. Res. Commun. 206*, 22−32.

Dauplais, M., Neumann, J. M., Pinkasfeld, S., Ménez, A., & Roumestand, C. (1995) *Eur. J. Biochem. 230*, 213−220.

Dufton, M. J., & Hider, R. C. (1991) in *Snake Venom* (Harvey, A. L., Ed.) pp 259−302, Pergamon Press, Inc., New York.

Evans, R. W., Williams, M. A., & Tinoco, J. (1987) *Biochem. J. 245*, 455−462.

Gatineau, E., Takechi, M., Bouet, F., Mansuelle, P., Rochat, H., Harvey, A. L., Montenay-Garestier, Th., & Ménez, A. (1990) *Biochemistry 29*, 6480−6489.

Gilquin, B., Roumestand, C., Zinn-Justin, S., Ménez, A., & Toma, F. (1993) *Biopolymers 33*, 1659−1675.

Harvey, A. L. (1985) *J. Toxicol., Toxin Rev. 4*, 41−69.

Harvey, A. L. (1991) in *Handbook of Natural Toxins* (Tu, A. T., Ed.) Vol. 5, pp 85−103, M. Dekker, Inc., New York.

Jeener, J., Meier, B. H., Bachman, P., & Ernst, R. R (1979) *J. Chem. Phys. 71*, 4546−4553.

Kini, R. M., & Evans, H. J. (1989) *Biochemistry 28*, 9209−9215.

Kohda, D., & Inagaki, F. (1992) *Biochemistry 31*, 11928−11939.

Kuchinka, E., & Seelig, J. (1989) *Biochemistry 28*, 4216−4221.

Le Goas, R., LaPlante, S. R., Mikou, A., Delsuc, M-A., Guittet, E., Robin, M., Charpentier, I., & Lallemand, J. Y. (1992) *Biochemistry 31*, 4867−4875.

Leroy, E., Mikou, A., Yang, Y., & Guittet, E. (1994) *J. Biomol. Struct. Dyn. 12*, 1−17.

Macura, S., & Ernst, R. R.(1980) *Mol. Phys. 41*, 95−117.

Marion, D., & Wüthrich, K. (1983) *Biochem. Biophys. Res. Commun. 113*, 967−974.

McLaughlin, S. (1977) *Curr. Topics Membr. Transp. 9*, 71−144.

Ménez, A., Gatineau, E., Roumestand, C., Harvey, A. L., Mouawad, L., Gliquin, B., & Toma, F. (1990) *Biochimie 72*, 575−588.

Ohshima, H., & Ohki, S. (1985) *Biophys. J. 47*, 673−678.

Pardi, A., Wagner, G., and Wüthrich, K. (1983) *Eur. J. Biochem. 137*, 445−454.

Piotto, M., Saudek, V., & Sklenár, V. (1992) *J. Biomol. NMR 2*, 661−665.

Roumestand, C., Gilquin, B., Trémeau, O., Gatineau, E., Mouawad, L., Ménez, A., & Toma, F. (1994) *J. Mol. Biol. 243*, 719−735.

Singhal, A. K., Chien, K.-Y., Wu, W., & Rule, G. S. (1993) *Biochemistry 32*, 8036−8044.

Stankowski, S., & Schwarz, G. (1990) *Biochim. Biophys. Acta 1025*, 164−172.

Sun, Y.-J., Wu, W., Chiang, C.-M., Hsin, A.-Y., & Hsiao, C.-D. (1996) *J. Biol. Chem.* (submitted).

Surewicz, W. K., Stepanik, T. M., Szabo, A. G., & Mantsch, H. H. (1988) *J. Biol. Chem. 263*, 786−790.

Takechi, M., Tanaka, Y., & Hayashi, K. (1985) *Biochem. Int. 11*, 795−802.

Wu, W., Li, Y., & Szabo, G. (1993) *FASEB J. 7*, A1235.

Wüthrich, K. (1986) *NMR of Proteins and Nucleic Acids*, Wiley-Interscience, New York.

BI952823K